HHS Public Access

Author manuscript

Int J Radiat Oncol Biol Phys. Author manuscript; available in PMC 2020 March 01.

Published in final edited form as:

Int J Radiat Oncol Biol Phys. 2019 March 01; 103(3): 697–708. doi:10.1016/j.ijrobp.2018.10.009.

AN ANTI-TUMOR IMMUNE RESPONSE IS EVOKED BY PARTIAL-VOLUME SINGLE DOSE RADIATION IN TWO MURINE MODELS

Ela Markovsky[1], **Sadna Budhu**[3], **Robert M. Samstein**[1], **Hongyan Li**[1], **James Russell**[2], **Zhigang Zhang**[4], **Esther Drill**[4], **Chloe Bodden**[1], **Qing Chen**[2], **Simon N. Powell**[1], **Taha Merghoub**[3], **Jedd D. Wolchok**[3], **John Humm**[2], **Joseph O. Deasy**[2], **Adriana Haimovitz-Friedman**[1,*]

[1]Department of Radiation Oncology, Memorial Sloan Kettering Cancer Center, New York, New York, United States

[2]Department of Medical Physics, Memorial Sloan Kettering Cancer Center, New York, New York, United States

[3]Parker Institute for Cancer Immunotherapy, Memorial Sloan Kettering Cancer Center, New York, New York, United States

[4]Department of Epidemiology and Biostatistics, Memorial Sloan-Kettering Cancer Center, New York, New York, United States

Abstract

Purpose: To study tumor growth delay resulting from partial irradiation in preclinical mouse models.

Methods and Materials: We investigated 67NR murine orthotopic breast tumors in both immunocompetent and nude mice. Treatment was delivered to 50% or 100% of the tumor using a 2×2 cm collimator on a micro-irradiator. Radiation response was modulated by treating with anti-CD8 and anti-ICAM antibodies. Similar experiments were performed using the less immunogenic Lewis Lung Carcinoma (LLC) mouse model. Tumor growth delay and gγH2AX phosphorylation were measured and immune response was assessed by immunofluorescence and flow cytometry at 1 and 7 days post-radiotherapy (RT). Tumor expression of cellular adhesion molecules was also measured at different times post-RT.

Results: Partial irradiation led to tumor responses similar to fully exposed tumors in immunocompetent mice, but not in nude mice. After a single dose of 10Gy, infiltration of $CD8^+$ T cells was observed, along with increased expression of ICAM. The response to 10Gy in hemi-

*Corresponding author: Adriana Haimovitz-Friedman, Department of Radiation Oncology, Memorial Sloan, Kettering Cancer Center, 1275 York Avenue, New York, NY 10065;; Telephone: 646-888-2172;; Fax: 646-422-0281;; a-haimovitz-friedman@ski.mskcc.org.

Disclusures

None

irradiated tumors was abrogated by treatment with either anti-CD8 or anti-ICAM antibodies. Similar responses were obtained in the less immunogenic LLC mouse model delivering 15Gy to half the tumor volume. Treatment with FTY720, a compound that inhibits T cell egress from lymph nodes, did not affect tumor response at the time of $CD8^+$ T cells infiltration in the non-irradiated area of the tumor, indicating that the most likely source of these cells is the irradiated portion of the hemi-irradiated tumors. In addition, a significant abscopal effect was observed after partial irradiation with a single dose of 10Gy in the 67NR model.

Conclusions: In these models, radiation controls tumor growth both directly through cell killing and indirectly through immune activation. This raises the possibility that this effect could be induced in the clinic.

Keywords

Radiation therapy; Immune activation; Endothelial cells; Cytotoxic T cells; ICAM

INTRODUCTION

Clinical radiation therapy aims to deliver an ablative dose of RT to the tumor while minimizing damage to adjacent normal tissue. To ensure full coverage of the tumor, treatment plans contain added margins to account for patient set-up uncertainties. While modern image guided radiation therapy (IGRT) allows for stereotactic delivery of high doses to the tumor (1,2), it is also associated with increased and sometimes devastating acute toxicities to adjacent tissues (3,4). To circumvent these risks, treatment plans are often more conservative at the interface between tumor and critical normal tissue, with the consequence that some of the tumor volume receives less than the prescription dose. It has been argued that these lower dose regions are possible sites of treatment failure.

According to classical radiobiology, tumor response is due to direct cell kill, caused by radiation-induced DNA damage produced within the primary radiation field. However, there is a growing amount of evidence that radiation also affects the tumor microenvironment and alters the balance of inflammatory signals in the tumor (5–11). The impact of host immune capability on RT response is well established in immunogenic murine tumor models (12). These effects have also been observed in distant tissues outside of the radiation field following hypofractionated or single high dose radiotherapy (SDRT), particularly when combined with systemic immune modulation therapies (7,13,14). Furthermore, previous studies by our group and others have shown that SDRT can invoke a biological mechanism of tumor lethality involving the tumor vasculature (15,16). In our previous work, we demonstrated that 15Gy induced rapid collapse of the tumor microvasculature due to surface translocation of acid sphingomyelinase (ASMase), and ceramide generation (15) in endothelial cells, leading to ischemia/reperfusion injury. The vasculature is a recognized target in cancer therapy and emerging data suggest that T cell-mediated effects on the tumor and stroma might be similarly linked to effects on the vessels, in part through the production of cytokines (17). It has been previously shown that the efficacy of the infiltrating $CD8^+$ T cells depends on their interaction with the tumor stroma (11,18–21).

Radiation oncologists carefully ensure that treatment plans provide full coverage of the tumor volume adding a margin, to account for set-up error and patient motion, in the belief that any part of the tumor missed by the radiation beams will lead to treatment failure. However, when the tumor location is close to a dose limiting tissue, the possibility of marginal misses arises. The radiobiological consequences of irradiation geometries that do not provide full tumor coverage has not been carefully studied, perhaps because it has always been assumed that such treatments would be wholly ineffectual. To replicate marginal miss geometry in a pre-clinical animal tumor model would be difficult due to the uncertainties in animal set-up in a microirradiator. Therefore, we decided to deliberately exaggerate the portion of unirradiated tumor and selected an irradiation geometry in which one half of the volume was blocked from the primary radiation field (Scheme 1). To ensure that the viable tumor was not preferentially located in the superior /inferior aspect of the tumor mass, the experiment was repeated to ensure no location bias. We examined the effect of hemi-tumor irradiation on tumor growth delay and on the microvascular and immune response within the irradiated and non-irradiated areas of the tumor. We studied the 67NR murine tumor model, previously demonstrated to be immunogenic (7) and the Lewis lung carcinoma model (LLC), which is considered to be less immunogenic and more radioresistant.

MATERIALS AND METHODS

Ethical statement

All animal experiments were performed according to the ethical guidelines, following a protocol approved by the Institutional Animal Care and Use Committee (IACUC). Animals were housed at the Research Animal Resource Center (RARC) of Memorial Sloan-Kettering Cancer Center (MSKCC). The facility is approved by the American Association for Accreditation of Laboratory Animal Care and is maintained in accordance with the regulations and standards of the United States Department of Agriculture and the Department of Health and Human Services, NIH.

Cell culture

67NR murine breast carcinoma cells, generously given by Dr. Ronald Blasberg (MSKCC), and Lewis Lung carcinoma cells (ATCC) were cultured in Dulbecco’s modified Eagle’s medium (DMEM) supplemented with 10% fetal bovine serum, 2 mM L-glutamine, 100U/ml penicillin, 100 μg/ml streptomycin and 0.25 μg/ml amphotericin B. Cells were kept in a humidified incubator at 37°C, in 5% CO_2.

Tumor inoculation

Balb/c, $C_{57}BL/_6$ or athymic nude mice were purchased from Jackson Laboratory (Bar Harbor, ME), and used at 12 weeks of age, in order to allow the immune system to mature. 67NR cells were orthotopically injected into the mammary fat pad at position 4 in the right side. For the bilateral tumors experiment, cells were injected at position 4 in both left and right sides. LLC cells were injected subcutaneously (s.c.) in the flank. 1.5×10^6 cells were injected in 50% Matrigel in PBS for both cell lines.

Irradiation procedure

Tumors (mean volume of 250mm^3) were irradiated with either 100% or 50% coverage using an XRAD 225C (Precision X-Ray, North Branford CT), with a 2×2cm collimator, at 225kV, 13mA, dose rate of approximately 3.5Gy/minute. The irradiation field was defined using GAF chromic film, and the mouse was positioned so that either all or half of the tumor was in the field (Scheme 1). The part of the tumor that was outside of the irradiation field (OF) received a dose of less than 5% of the primary in-field (IF) dose. After irradiation, mice were either observed for tumor response or euthanized at the time points stated to collect the tumors.

Antibody and drug treatment

Anti-CD8-alpha antibody (Mab/hybridoma 53–6.72) was obtained from the Antibody and Bioresource Core Facility at MSKCC. Antibody was injected intraperitoneally (i.p.) every 3 days, starting 3 days before irradiation and up to 6 days after irradiation, at 200 μg/animal/injection.

In vivo MAb anti-mouse CD54 (ICAM-1) and anti-mouse CD62E (E-selectin) (clones YN1/1.7.4 and 9A9, respectively) were obtained from Bioxcell (NH, USA). Antibody was injected i.p. 2, 16 and 48 hours after irradiation with 10Gy, at 300 μg/injection for ICAM-1 and 150 μg/injection for E-selectin.

FTY720, a compound that inhibits T cell egress from lymph nodes (22), was purchased from Sigma Aldrich (St Louis, MO, cat #SML0700) and administered i.p. once a day, at −2, −1 and on the day of irradiation, at 1.5 mg/kg.

Immunofluorescent staining

Staining was performed by MSKCC Molecular Cytology Core Facility using a Discovery XT processor (Ventana Medical Systems). Tumors were fixed with 10% formalin, embedded in paraffin and sectioned at 5μm thickness. Tissue sections were deparaffinized with EZPrep buffer followed by antigen retrieval with CC1 buffer (both Ventana Medical Systems). Sections were blocked for 30 minutes with Background Buster solution (Innovex).

Tumors that were 50% irradiated were cut with a scalpel along the edge of the irradiation field (marked on the skin of the mouse) prior to excision of the tumor and the irradiated and non-irradiated halves were processed separately.

Sections were incubated with primary antibodies (**anti-CD8**: eBiosciences, **anti-CD4**: R&D Systems, **anti-Meca-32**: DSHB, **anti-ICAM1**: R&D Systems, **anti-VCAM-1**: R&D Systems, **anti-E-Selectin**: R&D Systems, **anti-P-Selectin**: LSBio, **anti-γH2AX**: Millipore), followed by 60 minutes incubation with the appropriate biotinylated secondary antibody (goat anti-rat IgG (Vector labs), horse anti-goat IgG (Vector labs), goat anti-chicken IgY (Vector labs), goat anti-rabbit IgG (Vector labs), horse anti-mouse IgG (Vector labs). The detection was performed with Streptavidin-HRP D (part of DABMap kit, Ventana Medical Systems), followed by incubation with Tyramide Alexa Fluor 488 (Invitrogen) prepared

according to manufacturer instruction. After staining slides were counterstained with DAPI (Sigma Aldrich) for 10 minutes and coverslipped with Mowiol mounting media.

Imaging and analysis

Slides were imaged on a Pannoramic 250 slide scanner (3DHISTECH) at 40x resolution. Entire tissue sections were used for analysis. Threshold was adjusted to exclude background and stained regions were quantified using ImageJ.

Evaluation of infiltrating immune cells by flow cytometry

Tumors and tumor draining lymph nodes were excised 1 and 7 days post-RT and mechanically dissociated into single cell suspensions using 4μm cell strainers (Falcon). Cell suspensions were incubated in Fc block (anti-CD16 and anti-CD32 antibodies;; BD Biosciences) for 20 minutes on ice in FACS buffer (0.5% BSA and 2 mM EDTA in PBS), then incubated with fluorophore-conjugated antibodies against CD45, CD4, CD8 and PD-1 for 20 to 30 minutes on ice and washed three times with FACS buffer. For intracellular staining of Foxp3 and granzyme B, cells were fixed and permeabilized using the Foxp3 Staining Kit (eBioscience). Dead cells were excluded using the Fixable Viability Dye eFluor 506 (eBioscience). Samples were acquired on a 12-color LSR II flow cytometer, and data were analyzed with FlowJo software (Tree Star).

Statistical analysis

All statistical analysis was performed by the Biostatistics facility at MSKCC using SAS 9.4 (SAS Institute, Inc., Cary, NC, USA). For Fig. 1A, 1B, 2D, 3D, 4A, 5A, 5B, 5C and 6, the slope of the tumor growth curve for each animal was estimated using simple linear regression on all available data. Wilcoxon rank-sum tests were used to compare slopes or raw measurements (for figures 1D, 2A, 3B and 3D) between two treatment groups. Specifically, we implemented Monte Carlo estimation with 10,000 simulated data sets in the SAS NPar1Way Procedure to estimate two-sided exact Wilcoxon rank-sum P-values. The statistical significance level was set at alpha=0.05 (i.e., $P<0.05$) despite the multiple comparisons, in order not to inflate the Type II (false-negative) error rate in this exploratory study. Information on the number of repeats and number of mice in each experiment can be found in the figure legends. Error bars in the figures represent one standard error of the mean (SEM). P-values inside the figures are represented using asterisks as follows: * $P<0.05$, ** $P<0.005$, *** $P<0.001$.

RESULTS

Full or partial irradiation effects on tumor growth

The effect of hemi vs. full tumor irradiation was examined on an orthotopic murine 67NR breast cancer model, implanted in the mammary fat pad of immunocompetent Balb/c mice. Tumors were subjected to 10, 15 or 20Gy. Tumor responses were measured for non-irradiated, hemi-irradiated, and fully-irradiated tumors.

The expectation is that a hemi-irradiated tumor would undergo no more than 50% cell killing, and as a result its regrowth delay should not exceed one volume doubling time. This

is what was observed (0 of 15 67NR tumor cures) when the hemi-irradiation procedure was applied to tumors in nude mice (Fig.1A). It was further confirmed in a second MDA-MB-231 breast tumor model (0 of 16 mice hemi-irradiated tumors survived - data not shown). Surprisingly, when these experiments were conducted on the same tumor grown in immunocompetent Balb/c mice, hemi-irradiation resulted in several (5 of 15) tumor cures (Fig. 1B and supp. fig. S2). These cures cannot be explained by the therapeutic effects of the radiation alone.

There are two statistical issues with this result. First issue is the difference between what was observed between hemi-irradiated tumors and the expected response. As stated above, hemi-irradiated tumors should exhibit minimal growth delay and cures should be impossible. Nonetheless, we observed 5 of 15 tumor cures in 3 groups of hemi-irradiated mice. Secondly, there is the question of whether the hemi- and fully irradiated tumors display comparable tumor growth delays. Pooling the data for 3 repeat experiments (18 mice per group), we did not find a statistically significant difference between the hemi-irradiated (50%) and the fully (100%) irradiated tumors (see Fig S2B in the supplementary data). These data provide compelling support for an immunostimulatory component of radiation monotherapy.

A further difference was found in the dose response relationship for the fully (100%) irradiated tumors. In the nude mouse model, tumor growth delay increased with increasing dose, whereas in the Balb/c model the response was seemingly independent of dose, i.e. the 10 and 20Gy doses resulted in equivalent tumor growth delay. These data suggest that the anti-tumor effects of radiation are in part due to the involvement of functional T cells.

DNA damage response

Tumors were evaluated 1 hour after RT for γH2AX foci, a marker of DNA double strand breaks. A dose-dependent increase in γH2AX foci was observed in the irradiated parts of the tumor. The non-irradiated half of tumors had γH2AX foci levels similar to the controls (Fig. 1C and 1D). These results serve to confirm that the experimental setup was arranged correctly, and the tumor cells in the non-irradiated half did not receive a significant partial dose due to scatter.

Mice did not develop tumors upon rechallenge

Balb/c mice from previous experiments, that were tumor free for at least 90 days following 10Gy hemi-irradiation, were inoculated again with 67NR cells (n=6). None of these mice developed tumors up to 90 days after the second inoculation. These data support the involvement of the adaptive immune system and indicate that the mice developed a memory response to these tumors.

RT induces cytotoxic T cell infiltration

Infiltration of $CD8^+$ cytotoxic T cells into both the irradiated and non-irradiated parts of the tumor was examined 24 hours after 10Gy RT. Immune-fluorescent staining revealed a 3-fold amplification of $CD8^+$ T cells in the non-irradiated half of the tumor (Fig. 2A and 2B). This

finding was confirmed by flow cytometry (Fig. 2C). No significant infiltration of $CD4^+$ cells was observed in the non-irradiated half of the tumor (supp. fig. S3).

In the next set of experiments, using flow cytometry, we determined the T cell activation markers Granzyme B and PD-1 at different time points post-RT (supp. fig. S4). PD-1 is an early activation marker for T-cells (as well as an exhaustion marker in later stages). It can be used to identify antigen experienced T cells and exhausted T cells that have been reinvigorated after immunotherapies (23–25). Granzyme B is a cytolytic enzyme that is expressed by cytotoxic $CD8^+$ T cells. This molecule is essential for $CD8^+$ T cells to kill their target and is upregulated on activated T cells (26). In addition to the increase in $CD8^+$ T cells at 24 hours, there was a trending increase in $CD8^+$ T cells in both the irradiated and non-irradiated parts of tumor 7 days post-RT (supp. fig. S4). At 7 days, the $CD8^+$ T cells appeared to be more activated and displayed increased expression of Granzyme B and PD-1 in both the tumor and the draining LNs. This data suggests that T cells were efficiently primed in response to radiation in the hemi-irradiated tumors. Of note, we observed a decrease in the numbers of $CD8^+$ T cells in the nearest draining LNs in the fully-irradiated tumors (supp. fig. S4). Furthermore, we did not observe sufficient activation of $CD8^+$ T cells in these LNs 24 hours or 7 days post RT. No significant changes were observed within the myeloid cells in the non-irradiated half of tumor (supp. fig. S5).

Cytotoxic T cell depletion abrogates the hemi-irradiated tumor response

To confirm the role of $CD8^+$ T cells in the response to partial irradiation, Balb/c mice implanted with 67NR tumors were treated with a CD8 depleting antibody in combination with 10Gy RT. Depletion of $CD8^+$ T cells led to a faster tumor growth in all three groups treated with the antibody. Depletion of $CD8^+$ T cells strongly reduced tumor response to RT in the hemi-irradiated tumors and, to a lesser degree, in the fully-irradiated tumors (Fig. 2D), confirming the role of these cells in the anti-tumor response to RT. The tumor growth delay of hemi-irradiated tumors in mice treated with CD8 depleting antibody was comparable to the one observed in hemi-irradiated tumors in nude mice (Fig. 1A).

RT induces increase in endothelial adhesion molecules in the non-irradiated half of tumor

We further examined the levels of several molecules that are critical for endothelial-leukocyte interaction and thus T cell infiltration. There was a significant increase in ICAM expression after irradiation with 10Gy, which was most prominent in the non-irradiated part of the tumor (Fig. 3A, 3B). No significant changes were observed in other adhesion molecules (VCAM, E-selectin and P-selectin) in the non-irradiated parts of the tumor (supp. fig. S6 A, B and C).

Anti-ICAM treatment leads to an abrogation of the hemi-irradiated tumor response

The increased ICAM expression suggests an important role for ICAM in mediating $CD8^+$ T-cell infiltration to the non-irradiated part of the tumor. To further examine this mechanism, we injected Balb/c mice with an ICAM blocking antibody, 2, 16 and 48 hours following 10Gy RT. Treating mice with anti-ICAM led to a decreased anti-tumor response in hemi-irradiated tumors compared to the fully-irradiated tumors (Fig. 3C). Blocking E-selectin did not affect the response of the 50% irradiated tumors relative to the 100% irradiated tumors

(supp. fig. S6D). Anti-ICAM treatment lead to a corresponding reduction in the number of infiltrating $CD8^+$ T cells in the non-irradiated half of hemi-irradiated tumors 24 hours post RT, but did not affect their infiltration to the irradiated half (Fig. 3D).

Origin of the early infiltrating $CD8^+$ cells is not the draining LNs

There is significant $CD8^+$ T cells infiltration in the non-irradiated tumor volume following hemi-irradiation. To establish whether these T cells are coming from the draining LNs, we treated the mice with FTY720, a compound that inhibits the egress of T cells from LNs and reduces peripheral blood lymphocyte counts via inhibition of sphingosine-1-phosphate (22). Treatment with FTY720 had no effect on tumor response up to 7 days (Fig. 4A) while inducing a dramatic decrease of $CD8^+$ T cells in the blood, confirming that the FTY720 treatment was effective (Fig 4B). These results suggest that the origin of the early infiltrating $CD8^+$ T cells in the non-irradiated part of the tumor is the tumor periphery and/or the irradiated portion of the tumor but not the LNs or the circulation.

Approximately a week after RT, both hemi- and fully-irradiated tumors in the FTY720 treated groups began growing rapidly while in the non-treated groups, tumors remained small (Fig. 4A). This suggests that T cell egress from the LNs appears to be necessary for maintaining tumor control over the long term.

Given the inclusion of draining lymphatics in the 100% RT field and not the 50% RT field, it was important to assess whether the beneficial effect of additional RT coverage in the 100% group may be counteracted to some extent by negative effects on local immune response. We performed an experiment where the irradiation field was on the upper part of the hemi-irradiated tumor and therefore included the draining LN. Similar results were obtained as in the original experiments;; the hemi-irradiated and fully irradiated tumors had a similar response to 10Gy RT (supp. fig. S7).

Hemi-irradiation of Lewis lung tumor model

To test whether the initial RT-induced mechanism of tumor response was unique to the 67NR model, we examined the effect of hemi-irradiation on LLC implanted s.c. in the flank of $C_{57}BL/_6$ mice. In this model 15Gy was required to achieve adequate tumor response (Fig. 5A), and again both fully and hemi-irradiated tumors responded equally. Surprisingly, when the dose was increased to 20Gy, the hemi-irradiation effect disappeared. We would speculate that vascular damage in the tumor may interfere with the ability of the immune system to access unirradiated tissues.

Consistent with our 67NR data, depleting the $CD8^+$ T cell population both abolished the hemi-irradiation effect and reduced the response of the tumor to 100% exposure, thus demonstrating the role of the immune system in amplifying radiation effects and to some extent in the non-irradiated tumors. When an anti-ICAM antibody was given, there was a reduced anti-tumor response in the hemi-irradiated tumors, though blocking ICAM did not affect the response in fully irradiated tumors. These results indicate that ICAM expression and $CD8^+$ T cells are necessary to the hemi-irradiated response in the LLC model as well.

Response to RT in a contralateral tumor

After full or hemi-irradiation of orthotopic 67NR tumors with 10Gy, we examined the effect of RT on a contralateral non-irradiated tumor. 10Gy RT induced a significant tumor growth delay in the contralateral tumors, whether the treated tumor was fully or hemi-irradiated, but no tumor cures like in the primary tumor (Fig. 6).

DISCUSSION

Our data indicate that hemi-irradiation of the mouse tumor volume was sufficient for tumor control via a putative immuno-stimulatory mechanism. The immune response appeared mainly $CD8^+$ T cell-mediated, given that when the same experiment was performed in athymic mice, or in immunocompetent mice treated with CD8-depleting antibody, the hemi-irradiated tumors showed minimal tumor growth delay. There was a significant increase in $CD8^+$ T cells in the non-irradiated portion of the hemi-irradiated tumors 24 hours post-RT and this increase was shown to be ICAM-dependent. Complete depletion of $CD8^+$ T cells resulted in reduced tumor response immediately after RT (Fig. 2D) while blocking T cell egress from the LN only affected long-term response in the hemi-irradiated tumors (Fig. 4A). Hemi-irradiation of the tumor generated a significant abscopal effect in the collateral tumor (Fig. 6).

The immunomodulatory effects of radiation have been described in preclinical studies and anecdotally in clinical reports. Radiation has been shown to affect either directly or indirectly all key components that are critical for the development of a potent anti-tumor immune response. These include upregulation of tumor antigen release and its presentation in MHC I/II molecules (11,20), activation of T cells (12), activation of immunogenic cell death via upregulation of damage associated molecular patterns including calreticulin, ATP and HMGB1 (27–29), and chemokine and cytokine secretion within the tumor and draining lymph nodes promoting a pro-inflammatory infiltrate (6).

Immuno-stimulatory responses are usually described as abscopal effects (from the Latin *ab scopus*, away from target), potentially impacting not only unexposed portions of the irradiated tumors but also metastatic lesions distant from the irradiation site. The mechanisms behind this phenomenon are still the subject of investigation (7,8,30–36). An exciting recent study in patients showed that a combination of pembrolizumab with either partial or full irradiation resulted in a similar degree of tumor control (37,38), which the authors termed ADscopal (close to target) effect. These data are consistent with our work which show that partial irradiation could be immuno-stimulatory improving therapeutic outcome. Furthermore, our results showed that hemi-irradiation of a tumor on one flank induced a significant tumor response in a contralateral non-irradiated tumor as well. However, the response was less in the contralateral from the hemi-irradiated primary, demonstrating that the “ADscopal” response is stronger than the “abscopal” response. Further studies are necessary to investigate if the effect of RT on blood vessels that results in overexpression of ICAM and early infiltration of CD8+ T cells is unique to the hemi-irradiated tumors.

One novel aspect of our work was that the immune response was produced without addition of checkpoint inhibitors to the protocol. Demaria et al. demonstrated that a single dose of 8Gy in combination with checkpoint inhibitor immunotherapy was able to shrink both irradiated and non-irradiated bilateral 67NR tumors, via cytotoxic T cells (7). Numerous preclinical studies and several clinical trials have been reported demonstrating the potential synergy of immune checkpoint inhibitors and radiation (39–42).

It is important to note that the off-target effects and immune stimulation we observed were without any exogenous immune stimulation apart from irradiation. While recent studies have focused on demonstrating and understanding the synergy between immunotherapy and RT (40), understanding the mechanisms of the immuno-stimulatory properties of radiation alone are critical before optimizing synergy with other therapeutics. Leukocyte recruitment is a multistep process consisting of leukocyte rolling, adhesion and transmigration (43). Endothelial cell activation and ICAM surface expression is essential for leukocyte recruitment to sites of inflammation (44). Radiation has previously been implicated in the upregulation of endothelial adhesion molecules (45). We observed a higher level of ICAM in the non-irradiated half of the hemi-irradiated tumor. Blocking of ICAM led to decreased response in hemi-irradiated tumors, but not in fully irradiated tumors, confirming the important role of ICAM in this mechanism. A decreased response in hemi-irradiated tumors was also observed after using an anti-CD8 antibody to suppress $CD8^+$ T-cell activity. This decreased response was observed, even after administering anti-CD8 antibody to the 100% tumor irradiated cohort, implicating a contribution of the immune system to the treatment response of fully irradiated tumors “. Taken together, our data shows that elevated ICAM expression is critical to recruit $CD8^+$ T cells to the shielded tumor region and is necessary to achieve durable responses.

Our experiments with a second model, LLC, confirm that the findings are not unique to 67NR breast cancer or otherwise highly immunogenic tumors, and therefore may be applicable to a wide range of tumors. The hemi-irradiation responses in this model were likewise abrogated by anti-CD8 treatment.

The expected response of a hemi-irradiated tumor is that the tumor growth delay would resemble an unirradiated tumor differing by one tumor doubling time (~2–3 days). This expected result was observed when our experiments were performed in a nude mouse model. However, the exact same tumor cells grown in immunocompetent mice had a completely different outcome. The hemi-irradiated tumor response curves resembled more closely the 100% irradiated tumor than the unirradiated control animals with several tumor cures. Subsequent experiments demonstrated that this was an immune dependent response and that it is reproducible in more than one tumor model. This response is dependent on vascular adhesion molecules that mediate infiltration of cytotoxic T-cells, arriving from the irradiated part of the tumor or tumor periphery. Furthermore, hemi-irradiation of the primary tumor elicited a significant abscopal effect in the contralateral tumor.

The results raise the possibility that this effect could be induced in some human tumors. In fact, we have observed several instances in the clinic where partial irradiation of the tumor

both combined with immune checkpoint blockade or alone have resulted in complete responses in the tumor despite limited dose to parts of the tumor (38,46,47).

Supplementary Material

Refer to Web version on PubMed Central for supplementary material.

Acknowledgements

We would like to thank Steven Chmura from the department of Radiation and Cellular Oncology, University of Chicago Cancer Center, for stimulating discussions. This study was supported by R&D funds from the departments of Radiation Oncology and Medical Physics, by NCI Core Center grant P30 CA008748, and a shared-resources grant from the MSKCC Geoffrey Beene Cancer Research Center for the purchase of the X-Rad 225Cx Microirradiator (PI: JOD).

REFERENCES

1. Fuks Z, Kolesnick R. Engaging the vascular component of the tumor response. Cancer Cell 2005;;8:89–91. [PubMed: 16098459]
2. Greco C, Zelefsky MJ, Lovelock M, et al. Predictors of local control after single-dose stereotactic image-guided intensity-modulated radiotherapy for extracranial metastases. Int J Radiat Oncol Biol Phys 2011;;79:1151–1157. [PubMed: 20510537]
3. Kim DW, Cho LC, Straka C, et al. Predictors of rectal tolerance observed in a dose-escalated phase 1–2 trial of stereotactic body radiation therapy for prostate cancer. Int J Radiat Oncol Biol Phys 2014;;89:509–517. [PubMed: 24929162]
4. Murphy JD, Christman-Skieller C, Kim J, et al. A dosimetric model of duodenal toxicity after stereotactic body radiotherapy for pancreatic cancer. Int J Radiat Oncol Biol Phys 2010;;78:1420–1426. [PubMed: 20399033]
5. Azzam EI, de Toledo SM, Little JB. Stress signaling from irradiated to non-irradiated cells. Curr Cancer Drug Targets 2004;;4:53–64. [PubMed: 14965267]
6. Chakraborty M, Abrams SI, Coleman CN, et al. External beam radiation of tumors alters phenotype of tumor cells to render them susceptible to vaccine-mediated t-cell killing. Cancer Res 2004;;64:4328–4337. [PubMed: 15205348]
7. Demaria S, Ng B, Devitt ML, et al. Ionizing radiation inhibition of distant untreated tumors (abscopal effect) is immune mediated. Int J Radiat Oncol Biol Phys 2004;;58:862–870. [PubMed: 14967443]
8. Formenti SC, Demaria S. Systemic effects of local radiotherapy. Lancet Oncol 2009;;10:718–726. [PubMed: 19573801]
9. Gorski DH, Beckett MA, Jaskowiak NT, et al. Blockage of the vascular endothelial growth factor stress response increases the antitumor effects of ionizing radiation. Cancer Res 1999;;59:3374–3378. [PubMed: 10416597]
10. Mothersill C, Seymour C. Radiation-induced bystander and other non-targeted effects: Novel intervention points in cancer therapy? Curr Cancer Drug Tar 2006;;6:447–454.
11. Reits EA, Hodge JW, Herberts CA, et al. Radiation modulates the peptide repertoire, enhances mhc class i expression, and induces successful antitumor immunotherapy. J Exp Med 2006;;203:1259–1271. [PubMed: 16636135]
12. Stone HB, Peters LJ, Milas L. Effect of host immune capability on radiocurability and subsequent transplantability of a murine fibrosarcoma. J Natl Cancer Inst 1979;;63:1229–1235. [PubMed: 291749]
13. Dewan MZ, Galloway AE, Kawashima N, et al. Fractionated but not single-dose radiotherapy induces an immune-mediated abscopal effect when combined with anti-ctla-4 antibody. Clin Cancer Res 2009;;15:5379–5388. [PubMed: 19706802]
14. Schaue D, Ratikan JA, Iwamoto KS, et al. Maximizing tumor immunity with fractionated radiation. Int J Radiat Oncol Biol Phys 2012;;83:1306–1310. [PubMed: 22208977]

15. Garcia-Barros M, Paris F, Cordon-Cardo C, et al. Tumor response to radiotherapy regulated by endothelial cell apoptosis. Science 2003;;300:1155–1159. [PubMed: 12750523]
16. Park HJ, Griffin RJ, Hui S, et al. Radiation-induced vascular damage in tumors: Implications of vascular damage in ablative hypofractionated radiotherapy (sbrt and srs). Radiat Res 2012;;177:311–327. [PubMed: 22229487]
17. Bruno A, Pagani A, Pulze L, et al. Orchestration of angiogenesis by immune cells. Front Oncol 2014;;4:131. [PubMed: 25072019]
18. Gasser S, Orsulic S, Brown EJ, et al. The DNA damage pathway regulates innate immune system ligands of the nkg2d receptor. Nature 2005;;436:1186–1190. [PubMed: 15995699]
19. Santin AD, Hermonat PL, Ravaggi A, et al. Radiation-enhanced expression of e6/e7 transforming oncogenes of human papillomavirus-16 in human cervical carcinoma. Cancer 1998;;83:2346–2352. [PubMed: 9840534]
20. Sharma A, Bode B, Wenger RH, et al. Gamma-radiation promotes immunological recognition of cancer cells through increased expression of cancer-testis antigens in vitro and in vivo. PLoS One 2011;;6:e28217. [PubMed: 22140550]
21. Wan S, Pestka S, Jubin RG, et al. Chemotherapeutics and radiation stimulate mhc class i expression through elevated interferon-beta signaling in breast cancer cells. PLoS One 2012;;7:e32542. [PubMed: 22396773]
22. Brinkmann V, Billich A, Baumruker T, et al. Fingolimod (fty720): Discovery and development of an oral drug to treat multiple sclerosis. Nat Rev Drug Discov 2010;;9:883–897. [PubMed: 21031003]
23. Simon S, Labarriere N. Pd-1 expression on tumor-specific t cells: Friend or foe for immunotherapy? Oncoimmunology 2017;;7:e1364828. [PubMed: 29296515]
24. Gros A, Robbins PF, Yao X, et al. Pd-1 identifies the patient-specific cd8(+) tumor-reactive repertoire infiltrating human tumors. J Clin Invest 2014;;124:2246–2259. [PubMed: 24667641]
25. Huang AC, Postow MA, Orlowski RJ, et al. T-cell invigoration to tumour burden ratio associated with anti-pd-1 response. Nature 2017;;545:60–65. [PubMed: 28397821]
26. Afonina IS, Cullen SP, Martin SJ. Cytotoxic and non-cytotoxic roles of the ctl/nk protease granzyme b. Immunol Rev 2010;;235:105–116. [PubMed: 20536558]
27. Apetoh L, Ghiringhelli F, Tesniere A, et al. Toll-like receptor 4-dependent contribution of the immune system to anticancer chemotherapy and radiotherapy. Nat Med 2007;; 13:1050–1059. [PubMed: 17704786]
28. Golden EB, Apetoh L. Radiotherapy and immunogenic cell death. Semin Radiat Oncol 2015;;25:11–17. [PubMed: 25481261]
29. Green DJ, Pagel JM, Nemecek ER, et al. Pretargeting cd45 enhances the selective delivery of radiation to hematolymphoid tissues in nonhuman primates. Blood 2009;;114:1226–1235. [PubMed: 19515724]
30. Deloch L, Derer A, Hartmann J, et al. Modern radiotherapy concepts and the impact of radiation on immune activation. Front Oncol 2016;;6:141. [PubMed: 27379203]
31. Demaria S, Golden EB, Formenti SC. Role of local radiation therapy in cancer immunotherapy. JAMA oncology 2015;;1:1325–1332. [PubMed: 26270858]
32. Formenti SC, Demaria S. Combining radiotherapy and cancer immunotherapy: A paradigm shift. J Natl Cancer Inst 2013;;105:256–265. [PubMed: 23291374]
33. Kaminski JM, Shinohara E, Summers JB, et al. The controversial abscopal effect. Cancer Treat Rev 2005;;31:159–172. [PubMed: 15923088]
34. Lee Y, Auh SL, Wang Y, et al. Therapeutic effects of ablative radiation on local tumor require cd8+ t cells: Changing strategies for cancer treatment. Blood 2009;;114:589–595. [PubMed: 19349616]
35. Scholch S, Rauber C, Weitz J, et al. Tlr activation and ionizing radiation induce strong immune responses against multiple tumor entities. Oncoimmunology 2015;;4:e1042201. [PubMed: 26451314]
36. Stamell EF, Wolchok JD, Gnjatic S, et al. The abscopal effect associated with a systemic anti-melanoma immune response. Int J Radiat Oncol Biol Phys 2013;;85:293–295. [PubMed: 22560555]

37. Lemons JM, Luke JJ, Janisch L, et al. The adscopal effect? Control of partially irradiated versus completely irradiated tumors on a prospective trial of pembrolizumab and sbrt per nrg-br001. Int J Radiat Oncol Biol Phys 2017;;99:S87.

38. Luke JJ, Lemons JM, Karrison TG, et al. Safety and clinical activity of pembrolizumab and multisite stereotactic body radiotherapy in patients with advanced solid tumors. J Clin Oncol 2018:jC02017762229.

39. Hiniker SM, Chen DS, Reddy S, et al. A systemic complete response of metastatic melanoma to local radiation and immunotherapy. Transl Oncol 2012;;5:404–407. [PubMed: 23323154]

40. Sharabi AB, Lim M, DeWeese TL, et al. Radiation and checkpoint blockade immunotherapy: Radiosensitisation and potential mechanisms of synergy. Lancet Oncol 2015;;16:e498–509. [PubMed: 26433823]

41. Twyman-Saint Victor C, Rech AJ, Maity A, et al. Radiation and dual checkpoint blockade activate non-redundant immune mechanisms in cancer. Nature 2015;;520:373–377. [PubMed: 25754329]

42. Weichselbaum RR, Liang H, Deng L, et al. Radiotherapy and immunotherapy: A beneficial liaison? Nat Rev Clin Oncol 2017;;14:365–379. [PubMed: 28094262]

43. Springer TA. Traffic signals for lymphocyte recirculation and leukocyte emigration: The multistep paradigm. Cell 1994;;76:301–314. [PubMed: 7507411]

44. Yang L, Froio RM, Sciuto TE, et al. Icam-1 regulates neutrophil adhesion and transcellular migration of tnf-alpha-activated vascular endothelium under flow. Blood 2005;;106:584–592. [PubMed: 15811956]

45. Quarmby S, Kumar P, Kumar S. Radiation-induced normal tissue injury: Role of adhesion molecules in leukocyte-endothelial cell interactions. Int J Cancer 1999;;82:385–395. [PubMed: 10399956]

46. LaPlant Q, Deselm C, Lockney NA, et al. Potential abscopal response to dual checkpoint blockade in rcc after reirradiation using dose-painting sbrt. Pract Radiat Oncol 2017;;7:396–399. [PubMed: 28551390]

47. Azami A, Suzuki N, Azami Y, et al. Abscopal effect following radiation monotherapy in breast cancer: A case report. Mol Clin Oncol 2018;;9:283–286. [PubMed: 30155251]

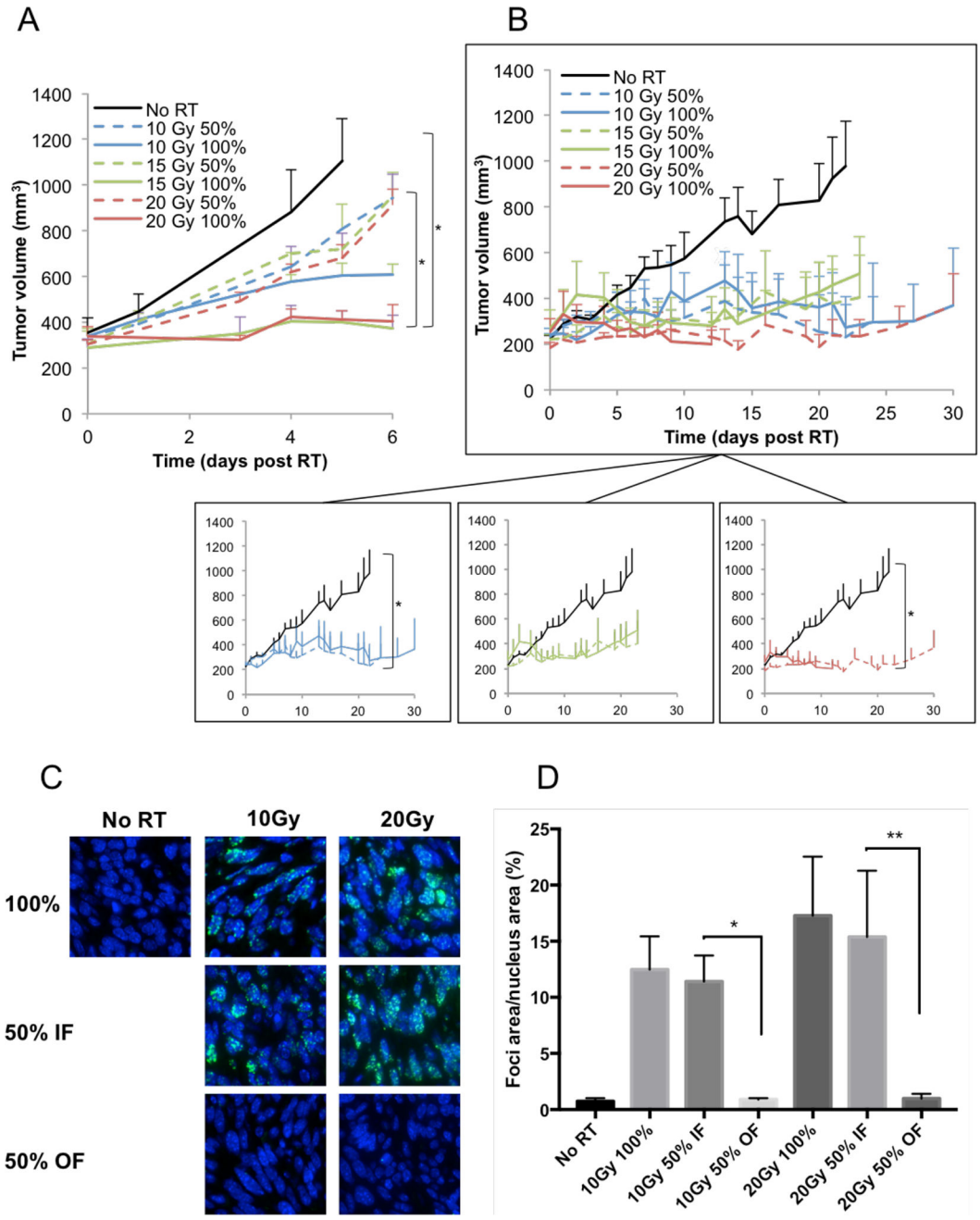

Figure 1 –.

(A) Athymic nude mice bearing orthotopic 67NR breast carcinoma tumors were irradiated with 10, 15 or 20Gy on either half (50%) or all (100%) of the tumor area. Experiment was done once, with 5 mice per group. In addition, an experiment on nude mice bearing MDA-MB-231 tumors was performed twice, with a total of 16 mice per group, with similar results. (B) Balb/c mice bearing orthotopic 67NR breast carcinoma tumors were irradiated with 10 15 or 20Gy on either half (50%) or all (100%) of the tumor area. A representative experiment is shown, with 5 mice per group. Experiment was done three times, with a total of 18 mice per group. (C) Representative γH2AX stained images with DAPI stained blue

nuclei for the unirradiated controls, 100% tumor coverage with 10 and 20Gy (row 1), in-field hemi-irradiated tumors (row 2 and out-of-field hemi-irradiated tumors (row 3). (D) Quantification of the γH2AX foci/nucleus from a representative experiment with 5 mice per treatment group. Experiment was done twice, with a total of 10 mice per treatment group.

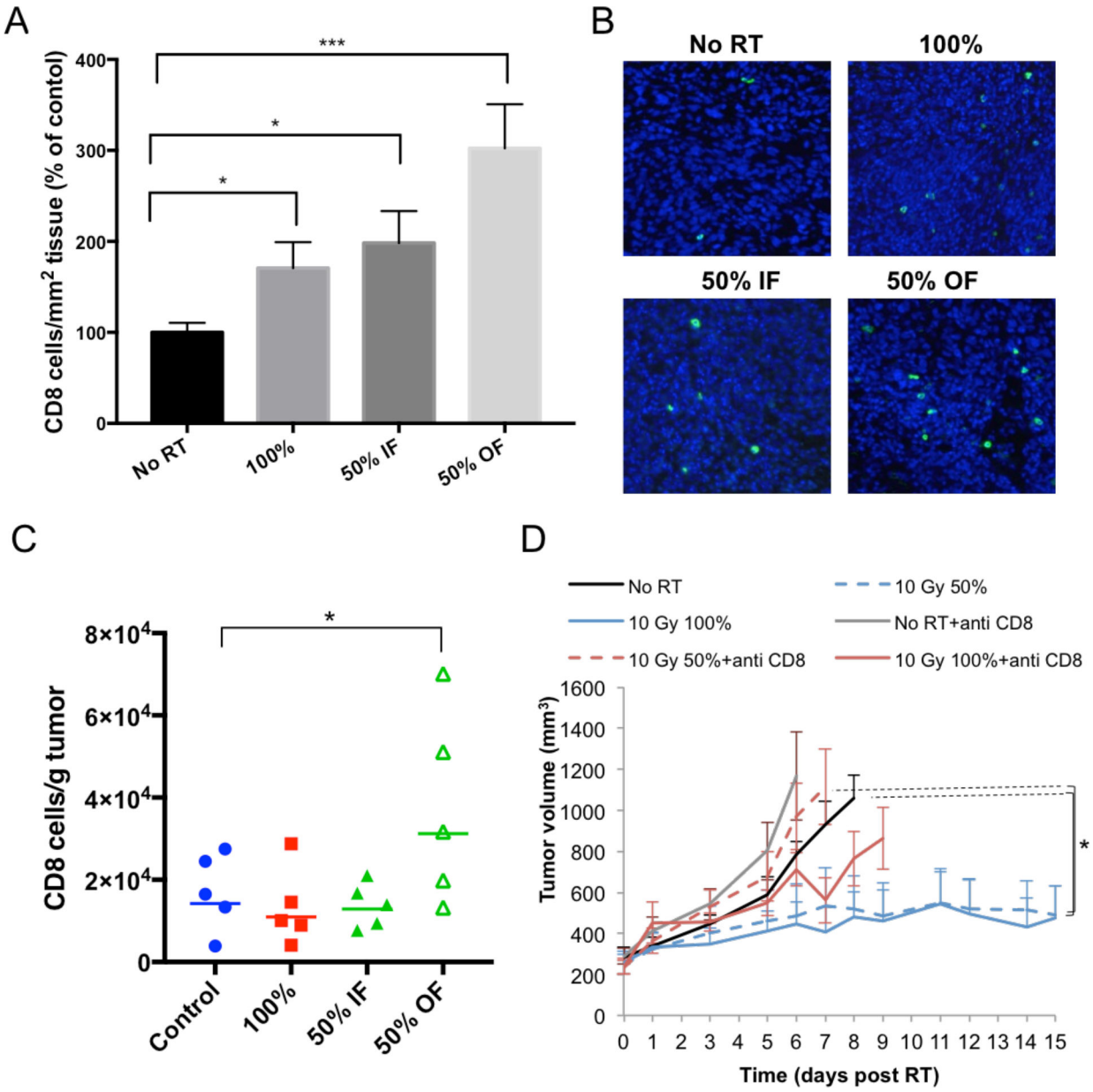

Figure 2 –.

Quantification (A) and example images (B) of the immunofluorescence staining of $CD8^+$ cells from the in-field and out-of-field hemi-irradiated tumors at 24 hours after irradiation with 10Gy RT (blue: DAPI, green: CD8). An average of 3 separate experiments is shown, with 21 mice per treatment group. (C) Quantification of $CD8^+$ cells from: unirradiated controls, 100% irradiated and from the in-field and out-of-field halves of the hemi-irradiated tumors. A representative experiment is shown, with 5 mice per group. Experiment was performed 3 times, with a total of 15 mice per group. (D) The effects of $CD8^+$ T cells depletion on 67NT tumor response to RT. $CD8^+$ T cells were depleted by four IP injections of anti-CD8 antibody, at a dose of 200μg/injection, starting 3 days before RT and 0, +3, +6 days after RT. Experiment was done once, with 5 mice per treatment group.

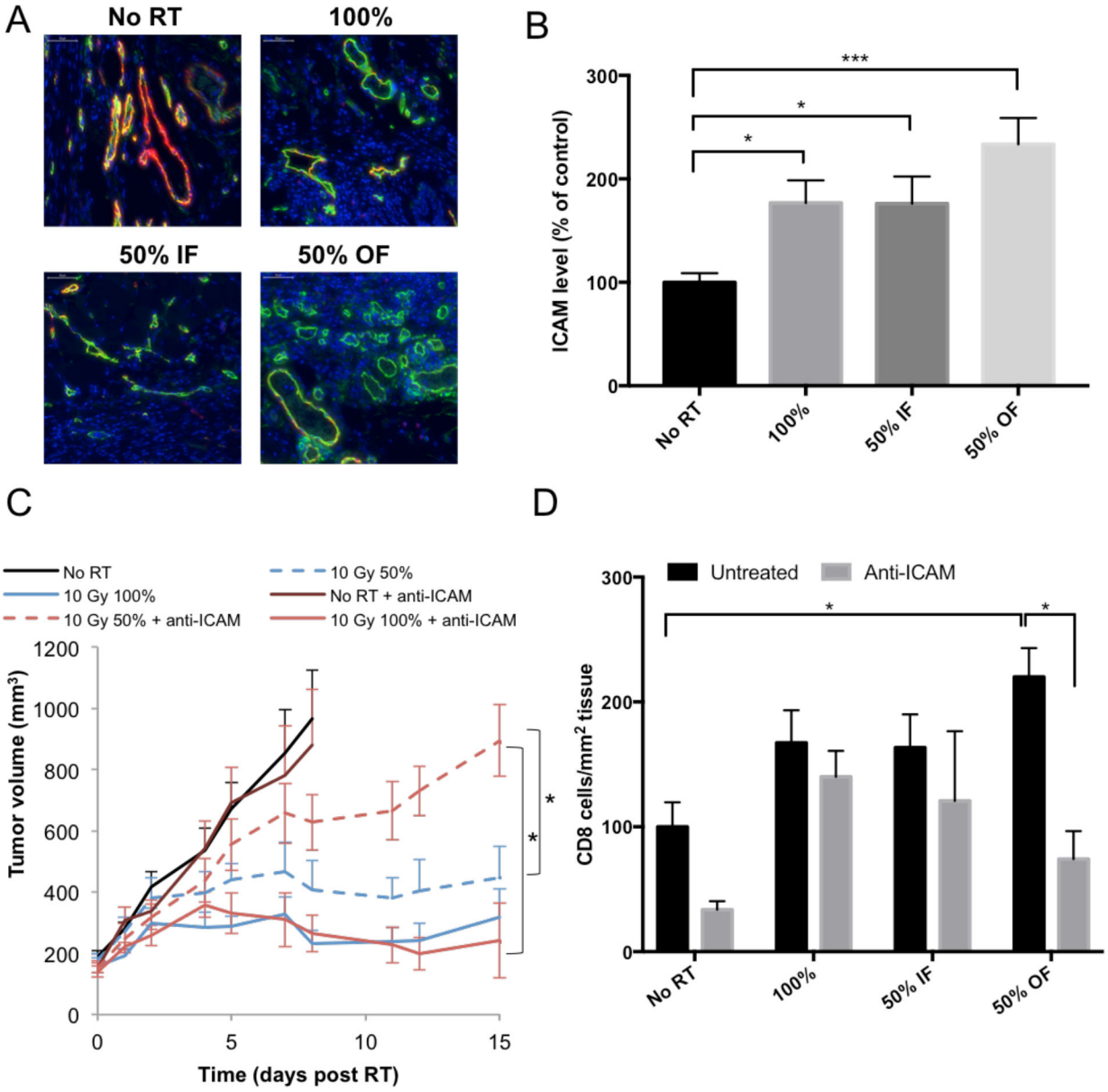

Figure 3 –.

(A) Representative images of ICAM expressed on blood vessels in the tumor (red: Meca-32, green: ICAM). An increase in ICAM expression was observed 24 hours post 10Gy RT in the out-of-field half of the tumor. (B) Quantitation of ICAM staining in tumors. An average of 3 separate experiments is shown, with a total of 15 mice per group. (C) The effects of blocking ICAM on 67NR tumor response to RT. IP injections of ICAM-blocking antibody were administered at a dose of 300μg/injection 2, 16 and 48 hours after RT. Experiment was done once, with 5 mice per group. (D) Effect of blocking ICAM on $CD8^+$ T cell infiltration following 10Gy hemi- or total irradiation and treatment with anti-ICAM antibody. IP injections of ICAM-blocking antibody were administered at a dose of 300μg/injection, 2 and 16 hours after RT. After 24 hours tumors were collected and $CD8^+$ cells were visualized using immunofluorescence. Experiment was done once, with 5 mice per group.

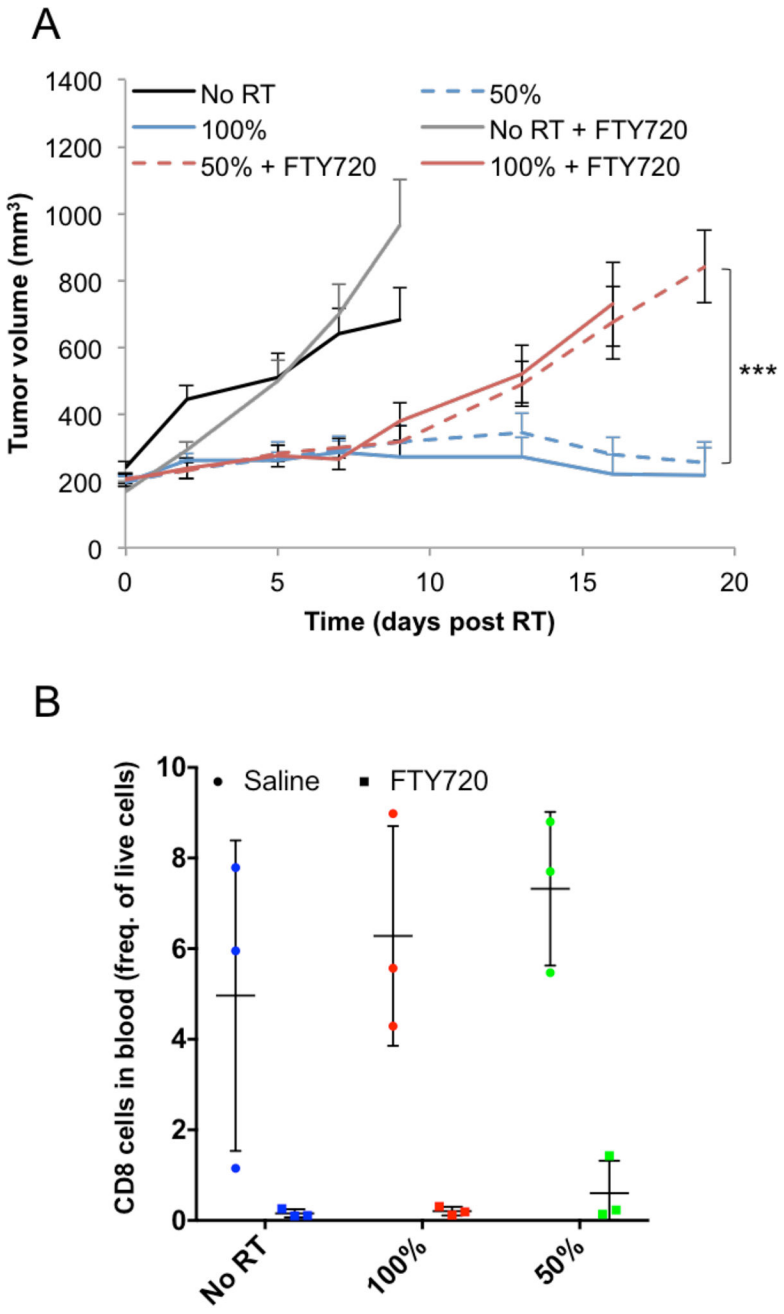

Figure 4 –.

(A) Effect of FTY720 treatment on tumor response. A representative experiment is shown, with 8 mice per group. Experiment was performed 3 times, with a total of 18 mice per group. (B) Effect of FTY720 treatment on $CD8^+$ T cells levels in the blood following 10Gy hemi- or total irradiation. A representative experiment is shown, with 3 mice per group. Experiment was performed 2 times, with a total of 6 mice per group. Measurement of the level of $CD8^+$ T cells in the blood confirmed FTY720 activity.

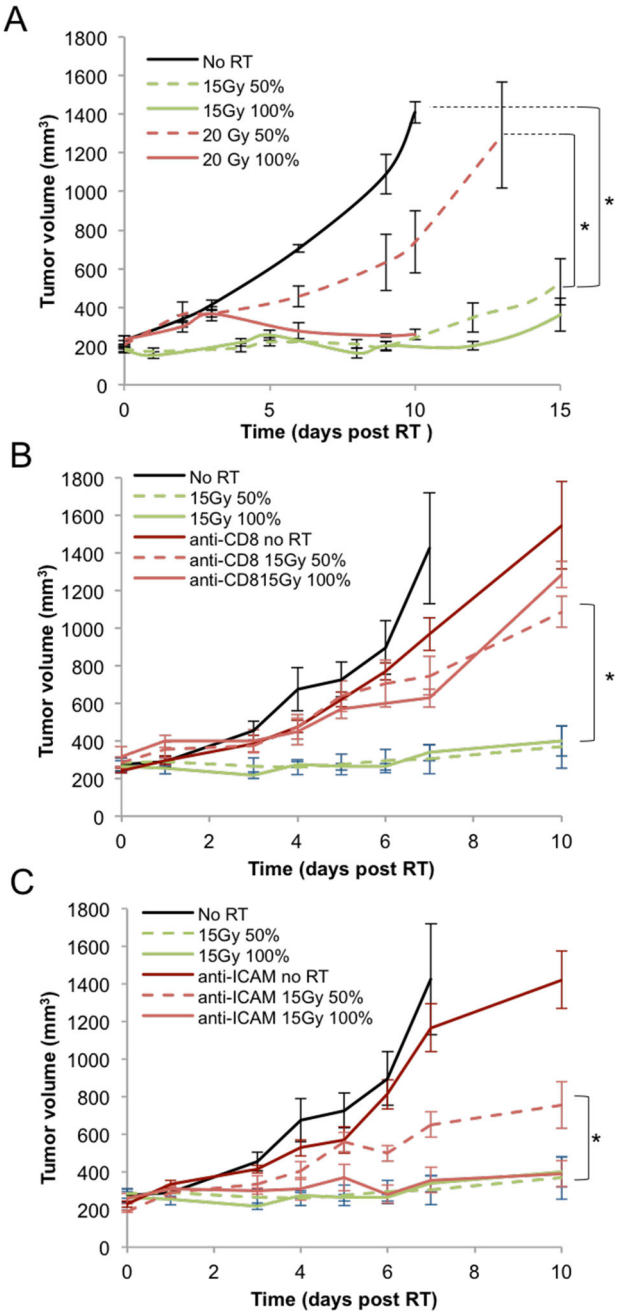

Figure 5 –.

(A) Tumor growth delay curves for C57BL/6 mice bearing flank subcutaneous LLC lung tumors after receiving hemi- or total irradiation with 15 or 20Gy. A representative experiment is shown, with 5 mice per treatment group. Experiment was performed 3 times, with 15 mice per treatment group. (B) Same as (A) but showing the effects of $CD8^+$ T cells depletion on LLC tumor response to RT. $CD8^+$ T cells were depleted by four IP injections of anti-CD8 antibody, at a dose of 200 μg/injection, starting 3 days before RT and 0, +3, +6 days after RT. Experiment was done once, with 5 mice per group. (C) Same as (A) but showing the effects of blocking ICAM on LLC tumor response to RT. IP injections of

ICAM-blocking antibody were administered at a dose of 300μg/injection 2, 16 and 48 hours after RT. Experiment was done once, with 5 mice per group.

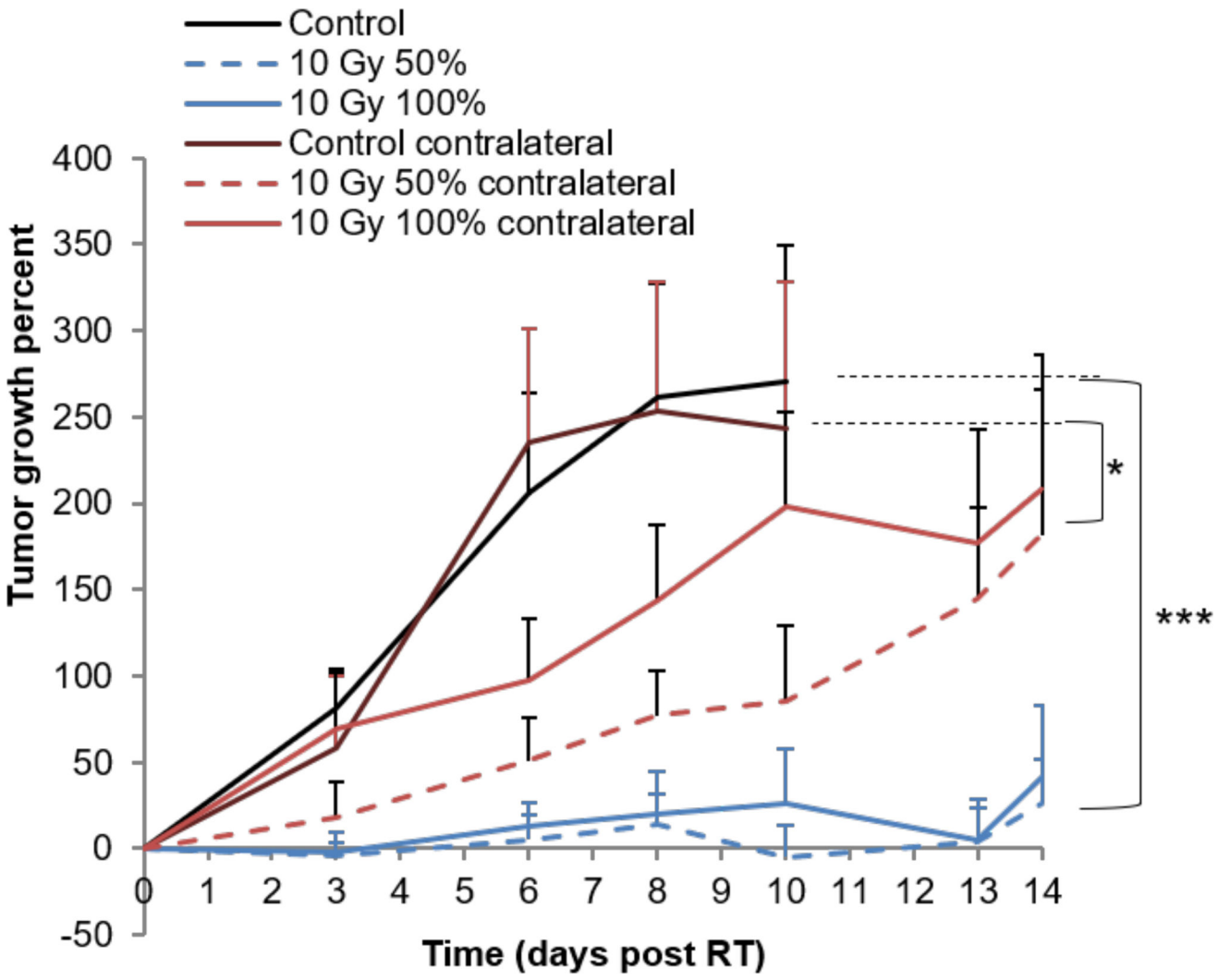

Figure 6 –.

(A) Tumor growth delay curves for bilateral orthotopic 67NR breast carcinoma tumors. Tumors were grown in each side of Balc/c mice and only the tumors on the right side received hemi- or total irradiation to either 10 or 20Gy. The tumor on the contralateral side of the animal, was completely outside of the field of the primary radiation beam. A representative experiment is shown, with 8 mice in the no RT group, 10 mice in 50% RT group and 5 mice in 100% RT group. Experiment was done 3 times, with a total of 17 mice per group in No RT and 50% groups and 10 mice in 100% group.